Growth of sparse arrays of narrow GaN nanorods hosting spectrally stable InGaN quantum disks

Yen-Ting Chen,[1] Wen-Che Tsai,[2] Wen-Yen Chen,[3] Ching-Lien Hsiao,[4] Hsu-Cheng Hsu,[4] Wen-Hao Chang,[2] Tzu-Min Hsu,[3] Kuei-Hsien Chen,[5,6] and Li-Chyong Chen[4,*]

[1]*Taiwan International Graduate Program, Institution of Atomic and Molecular Sciences, Academia Sinica, 10617, Taipei, Taiwan*
[2]*Department of Electrophysics, National Chiao Tung University, 30010, Hsinchu, Taiwan*
[3]*Department of Physics, National Central University, 32054, Chungli, Taiwan*
[4]*Center for Condensed Matter Sciences, National Taiwan University, 10617, Taipei, Taiwan*
[5]*Institute of Atomic and Molecular Sciences, Academia Sinica, 10617, Taipei, Taiwan.*
[6]*chenkh@pub.iams.sinica.edu.tw*
[*]*chenlc@ntu.edu.tw*

Abstract: Wafer-scale production of single InGaN quantum disks (QD) in-a-nanorod array with small rod diameter (> 9 nm) and low rod-density (< 10^8 cm^{-2}) has been achieved without extensive processing steps. Excitation power-dependent μPL spectrum of single QD reveals multi-excitonic peak with 0.75 meV blue-shift for 3 orders of magnitude increasing power, indicating the present system is spectrally stable and nearly free of quantum-confined Stark effects, due possibly to the strain relaxation induced by free surface of small rod diameters. The fully polarized emissions, a high working temperature (180 K), low rod density and good alignment, render this system promising as a potential quantum photon source.

©2012 Optical Society of America

OCIS codes: (160.6000) Semiconductor materials; (160.4236) Nanomaterials; (250.5590) Quantum-well, -wire and -dot devices.

References and links

1. S. Kako, C. Santori, K. Hoshino, S. Götzinger, Y. Yamamoto, and Y. Arakawa, "A gallium nitride single-photon source operating at 200 K," Nat. Mater. **5**(11), 887–892 (2006).
2. J. Ristić, E. Calleja, A. Trampert, S. Fernández-Garrido, C. Rivera, U. Jahn, and K. H. Ploog, "Columnar AlGaN/GaN nanocavities with AlN/GaN Bragg reflectors grown by molecular beam epitaxy on Si(111)," Phys. Rev. Lett. **94**(14), 146102 (2005).
<jrn>3. J. Renard, R. Songmuang, C. Bougerol, B. Daudin, and B. Gayral, "Exciton and biexciton luminescence from single GaN/AlN quantum dots in nanowires," Nano Lett. **8**(7), 2092–2096 (2008).</jrn>
4. R. Bardoux, A. Kaneta, M. Funato, Y. Kawakami, A. Kikuchi, and K. Kishino, "Positive binding energy of a biexciton confined in a localization center formed in a single InxGa$_{1-x}$N/GaN quantum disk," Phys. Rev. B **79**(15), 155307 (2009).
5. M. J. Holmes, Y. S. Park, J. H. Warner, and R. A. Taylor, "Quantum confined Stark effect and corresponding lifetime reduction in a single In$_x$Ga1-xN quantum disk," Appl. Phys. Lett. **95**(18), 181910 (2009).
6. L. F. Zagonel, S. Mazzucco, M. Tencé, K. March, R. Bernard, B. Laslier, G. Jacopin, M. Tchernycheva, L. Rigutti, F. H. Julien, R. Songmuang, and M. Kociak, "Nanometer scale spectral imaging of quantum emitters in nanowires and its correlation to their atomically resolved structure," Nano Lett. **11**(2), 568–573 (2011).
7. F. Glas, "Critical dimensions for the plastic relaxation of strained axial heterostructures in free-standing nanowires," Phys. Rev. B **74**(12), 121302 (2006).
8. H. Sekiguchi, K. Kishino, and A. Kikuchi, "Emission color control from blue to red with nanocolumn diameter of InGaN/GaN nanocolumn arrays grown on same substrate," Appl. Phys. Lett. **96**(23), 231104 (2010).
9. H. Schömig, S. Halm, A. Forchel, G. Bacher, J. Off, and F. Scholz, "Probing individual localization centers in an InGaN/GaN quantum well," Phys. Rev. Lett. **92**(10), 106802 (2004).
10. C. C. Chen, C. C. Yeh, C. H. Chen, M. Y. Yu, H. L. Liu, J. J. Wu, K. H. Chen, L. C. Chen, J. Y. Peng, and Y. F. Chen, "Catalytic growth and characterization of gallium nitride nanowires," J. Am. Chem. Soc. **123**(12), 2791–2798 (2001).

#165391 - $15.00 USD Received 23 Mar 2012; revised 27 Apr 2012; accepted 11 Jun 2012; published 2 Jul 2012

11. R. Calarco, R. J. Meijers, R. K. Debnath, T. Stoica, E. Sutter, and H. Lüth, "Nucleation and growth of GaN nanowires on Si(111) performed by molecular beam epitaxy," Nano Lett. **7**(8), 2248–2251 (2007).
12. K. A. Bertness, A. Roshko, N. A. Sanford, J. M. Barker, and A. Davydov, "Spontaneously grown GaN and AlGaN nanowires," J. Cryst. Growth **287**(2), 522–527 (2006).
13. J. Claudon, J. Bleuse, N. S. Malik, M. Bazin, P. Jaffrennou, N. Gregersen, C. Sauvan, P. Lalanne, and J. M. Gerard, "A highly efficient single-photon source based on a quantum dot in a photonic nanowire," Nat. Photonics **4**(3), 174–177 (2010).
14. S. Amloy, Y. T. Chen, K. F. Karlsson, K. H. Chen, H. C. Hsu, C. L. Hsiao, L. C. Chen, and P. O. Holtz, "Polarization-resolved fine-structure splitting of zero-dimensional In(x)Ga(1-x)N excitons," Phys. Rev. B **83**(20), 201307 (2011).
15. M. Sénès, K. L. Smith, T. M. Smeeton, S. E. Hooper, and J. Heffernan, "Strong carrier confinement in InxGa1-xN/GaN quantum dots grown by molecular beam epitaxy," Phys. Rev. B **75**(4), 045314 (2007).
16. A. F. Jarjour, R. A. Oliver, A. Tahraoui, M. J. Kappers, C. J. Humphreys, and R. A. Taylor, "Control of the oscillator strength of the exciton in a single InGaN-GaN quantum dot," Phys. Rev. Lett. **99**(19), 197403 (2007).
17. A. Dousse, J. Suffczyński, A. Beveratos, O. Krebs, A. Lemaître, I. Sagnes, J. Bloch, P. Voisin, and P. Senellart, "Ultrabright source of entangled photon pairs," Nature **466**(7303), 217–220 (2010).
18. C. Chèze, L. Geelhaar, O. Brandt, W. M. Weber, H. Riechert, S. Munch, R. Rothemund, S. Reitzenstein, A. Forchel, T. Kehagias, P. Komninou, G. P. Dimitrakopulos, and T. Karakostas, "Direct comparison of catalyst-free and catalyst-induced GaN nanowires," Nano Res. **3**(7), 528–536 (2010).
19. O. Moriwaki, T. Someya, K. Tachibana, S. Ishida, and Y. Arakawa, "Narrow photoluminescence peaks from localized states in InGaN quantum dot structures," Appl. Phys. Lett. **76**(17), 2361–2363 (2000).
20. V. D. Kulakovskii, G. Bacher, R. Weigand, T. Kummell, A. Forchel, E. Borovitskaya, K. Leonardi, and D. Hommel, "Fine structure of biexciton emission in symmetric and asymmetric CdSe/ZnSe single quantum dots," Phys. Rev. Lett. **82**(8), 1780–1783 (1999).
21. S. Amloy, K. F. Karlsson, T. G. Andersson, and P. O. Holtz, "On the polarized emission from exciton complexes in GaN quantum dots," Appl. Phys. Lett. **100**(2), 021901 (2012).
22. C. H. Bennett, "Quantum cryptography using any two nonorthogonal states," Phys. Rev. Lett. **68**(21), 3121–3124 (1992).
23. C. W. Hsu, A. Lundskog, K. F. Karlsson, U. Forsberg, E. Janzén, and P. O. Holtz, "Single excitons in InGaN quantum dots on GaN pyramid arrays," Nano Lett. **11**(6), 2415–2418 (2011).
24. J. Kalden, C. Tessarek, K. Sebald, S. Figge, C. Kruse, D. Hommel, and J. Gutowski, "Electroluminescence from a single InGaN quantum dot in the green spectral region up to 150 K," Nanotechnology **21**(1), 015204 (2010).
25. K. Sebald, H. Lohmeyer, J. Gutowski, T. Yamaguchi, and D. Hommel, "Micro-photoluminescence studies of InGaN/GaN quantum dots up to 150 K," Phys. Status Solidi, B Basic Res. **243**(7), 1661–1664 (2006).

1. Introduction

A nitride localized emission center (LC) is a desirable candidate as a single photon source owing to its robustness, sharp emission spectra, and tolerance to temperatures as high as 200 K [1]. Recently, by using the structure of a quantum disk (QD) embedded in a nanorod/nanowire grown by MBE [2–6], one can take advantage of the perfect crystal quality and the elastic strain relaxation of the free rod surfaces [7]. In the most-often reported GaN-QD/AlN-barrier system, the limit of UV emission in fiber communication and the difficulty of p-doping the AlN barrier layer are the main obstacles. On the other hand, InGaN is the material well-known for its visible-light emission in the nitride family. GaN as the barrier layer is also mature in the industry for p-doping. Therefore, from the perspective of quantum device-fabrication of next generation, the growth of an InGaN-QD/GaN-barrier system is a crucial step for the visible/infrared-light single photon source.

Several issues remain unsolved in the reported QD-in-a-rod system. A too high rod density (from 10^{10} to 10^{11} cm^{-2}) leads to a too high LC density [3, 5, 8], while the large rod diameter (> 50 nm), compared to the exciton Bohr radius of 3 to 11 nm in this material, leads to multiple LCs formed within a single rod. Debates as to whether the behavior of the exciton inside is due to quantum-well or quantum-dot behavior [3, 5, 9] also exist. The effect of strain relaxation induced by free surfaces will be reduced for samples with a large diameter. Meanwhile, wire-alignment has been long-time a challenge for both vapor-liquid-solid (VLS)-wires [10] and MBE-wires/rods [11, 12] . The optical collection efficiency will be much enhanced from the top of aligned nanorods [13].

In this study, single InGaN QDs was grown by MBE embedded in small diameter GaN nanorod in order to overcome the abovementioned issues. Radio frequency plasma-assisted

#165391 - $15.00 USD Received 23 Mar 2012; revised 27 Apr 2012; accepted 11 Jun 2012; published 2 Jul 2012
(C) 2012 OSA

molecular beam epitaxy (SVTA Model SVT-V-2) was used for the growth of InGaN QD and GaN nanorods on Si(111) substrate [14]. The size of the substrate is 4x4 cm. After substrate degassing in the growth chamber by heating up to 900°C, and cooling down to 500 °C, a 7x7 RHEED pattern was observed. A thin AlN nucleation layer was grown on top of the silicon substrate. GaN nanorods with lengths from 1 to 4 μm were then grown under N-rich conditions (3.5 sccm) at 750 °C. At the very end of the growth, 2 nm InGaN QD and a 5 nm thick GaN capping were subsequently grown.

2. Scheme and structure

The schematic structure and morphology are depicted in Fig. 1(a). Isolated nanorods were grown along the [0001] direction and well aligned. After dispersion on a carbon-coated copper mesh, crystal structure and composition of the QD and nanorod were analyzed by the transmission electron microscopy (TEM) (JEOL JEM-2100, 200KV) and accompanying scanning transmission electron microscopy with energy-dispersive X-ray spectroscopy (STEM-EDX) (Oxford INCATM Microsystem) technique, as shown in Fig. 1(b). The morphologies of the as grown samples are studied by scanning electron microscopy (SEM) as shown in Fig. 1(c). Statistically, the average rod diameter is 18 nm and 9 nm is the minimum. A sample as long as 4 μm has been grown under the preservation of uniform, non-tapered hexagonal shaped geometries. The self-induced growth structure features two parts: the upper narrow nanorods and the simultaneously grown underlying nanocolumns. The nanorods were found to appear at the initial stage of growth, and became elongated much faster than the columnar part during the growth with the diffusion-induced mechanism [11]. The lowest density among the batch of our samples is 9.66×10^{7} cm^{-2}, which is more than two orders of magnitude lower than typical SK quantum dots reported [15, 16]. In the literature, efforts have been reported to isolate emission peaks in order to circumvent the problem of a dot density that is too high to obtain single dot emission. These efforts include the use of post-treatment such as etching, nano-apertures made from electron beam lithography, and nonlinear optical technologies [15, 16]. The present structure thus provides an intrinsic advantage in emission isolation, by forming low density QD structures with high quantum efficiency, readily achieved from single bottom-up approach. Additionally, the low rod density and good alignment enable us to coat the rod with a high refractive-index outer shell with a thickness equal to the QD-emission wavelength (larger than 400 nm) and still remained isolated. Therefore, this structure shows a unique potential toward a microcavity-enhanced [13, 17] single photon source.

#165391 - $15.00 USD Received 23 Mar 2012; revised 27 Apr 2012; accepted 11 Jun 2012; published 2 Jul 2012
(C) 2012 OSA

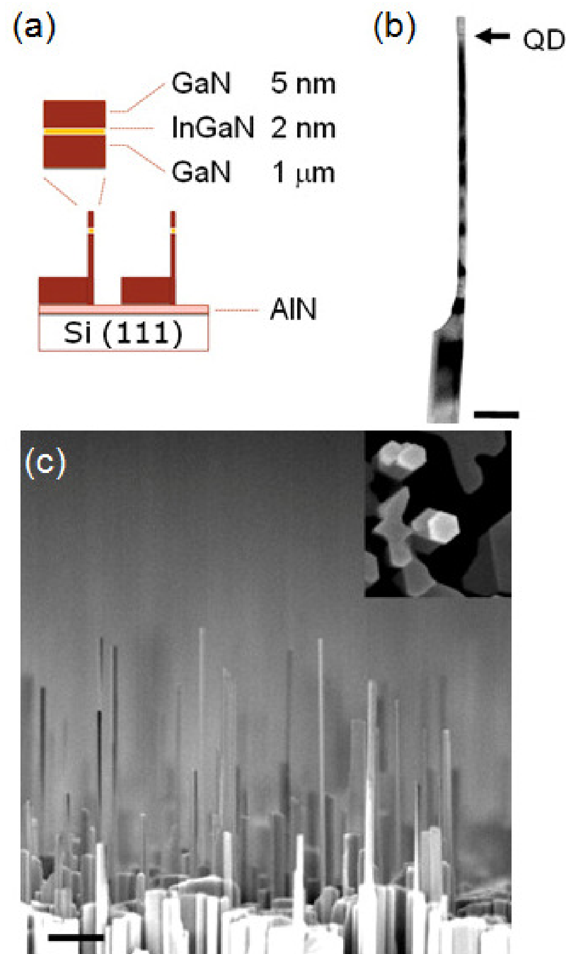

Fig. 1. Schematic illustration and morphology of InGaN QD in GaN nanorod. (a) Narrow GaN nanorods were grown on top of the Si(111) substrate and AlN nucleation layer by using MBE. The structure was divided into upper narrow nanorods and underlying columns.. A single 2 nm thick InGaN QD and a 5 nm GaN cap were grown on top of the GaN nanorod. The schematic is not to scale. (b) Transmission electron microscopy (TEM) bright field image of a single rod. The scale bar is 100 nm. A nanorod of 1 μm long was grown simultaneously with the underlying column and shared a common edge. The rod diameter shrinks 10 times from the columnar part to the rod part. The rod reveals almost no tapering effect after long-time growth. The QD is formed at the end of the rod (c) High resolution SEM image shows straight, well-aligned, uniform QD in-a-rod structure and underlying columns. The scale bar is 200 nm. The shapes of rods are hexagonal as shown in the inset.

3. Structural characterization

High resolution TEM was performed in order to investigate the detailed crystal structure (as shown in Fig. 2(a) to 2(c)). The position of the InGaN QD in the rod could be identified and was found to be properly located. No extended defects were found both for the nanorod and the QD in the nanorod, which are observable in some of the traditional strain-induced SK quantum dots embedded in the thin film. We attribute this phenomenon to the free-surface relaxation characteristic of this small diameter-structure [7]. However, stacking faults can be observed at the underlying parts of thick columns, as commonly observed in the MBE-grown GaN columns [18]. It indicates that the formation of stacking faults is suppressed during the growth of small-diameter rod. This self-suppressed formation of stacking fault makes this

#165391 - $15.00 USD Received 23 Mar 2012; revised 27 Apr 2012; accepted 11 Jun 2012; published 2 Jul 2012
(C) 2012 OSA

structure suitable as a building block for nano-scale device fabrication. STEM-EDX is used to investigate the amount of indium in the QD. It shows 10.03% molar ratio compared to that of gallium, as shown in Fig. 2(d). Also, the narrowest rod observed is 9 nm in diameter, as shown in Fig. 2(e).

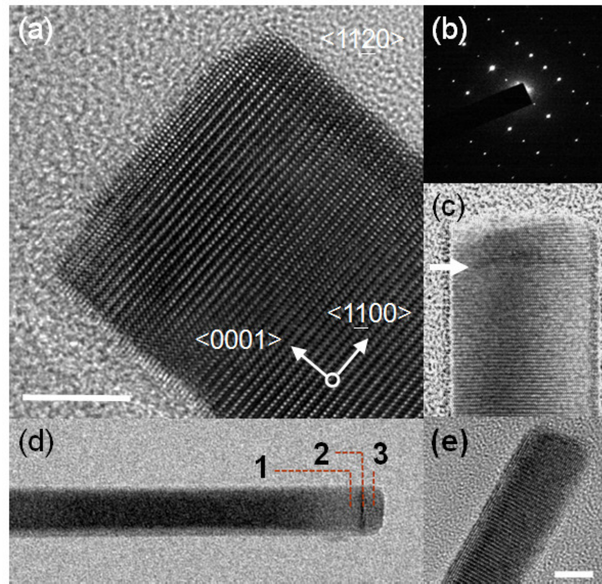

Fig. 2. Structural investigation of single InGaN QD in GaN nanorod by HRTEM and STEM-EDX. (a) Clear diffraction pattern of the wurtzite lattice with no dislocation or extended defect indicates high structural quality for both GaN and InGaN. The scale bar is 5 nm. (b) Selected area diffraction (SAD) pattern of the rod in (a). (c) TEM image of the *same* rod of (a) with the lower magnification shows the InGaN black stripe (pointed by arrow) along the radial direction. It indicates the position of the 2 nm InGaN QD and the thickness of capping GaN. (d) STEM-EDX investigation shows 2.93%, 10.03%, and 3.12% In/Ga molar ratio of InGaN QD when focusing the electron beam on the nanorod(1), QD(2), and the cap(3) respectively. (e) Nanorods are grown with a smallest diameter of 9 nm. The scale bar is 5 nm.

4. Optical characterization

Optical characterizations were performed on the *as grown* samples in order to determine if single QD emission behavior can be observed thanks to low-rod density, as shown in Fig. 3(a). It was performed with a μPL setup and with a continuous flow cryostat (Janis SuperTran) with different temperature. A 325 nm line He-Cd laser and a 0.75-m grating monochromator combined with a liquid nitrogen-cooled charge-coupled device (CCD) camera was used in the observation.

#165391 - $15.00 USD Received 23 Mar 2012; revised 27 Apr 2012; accepted 11 Jun 2012; published 2 Jul 2012
(C) 2012 OSA

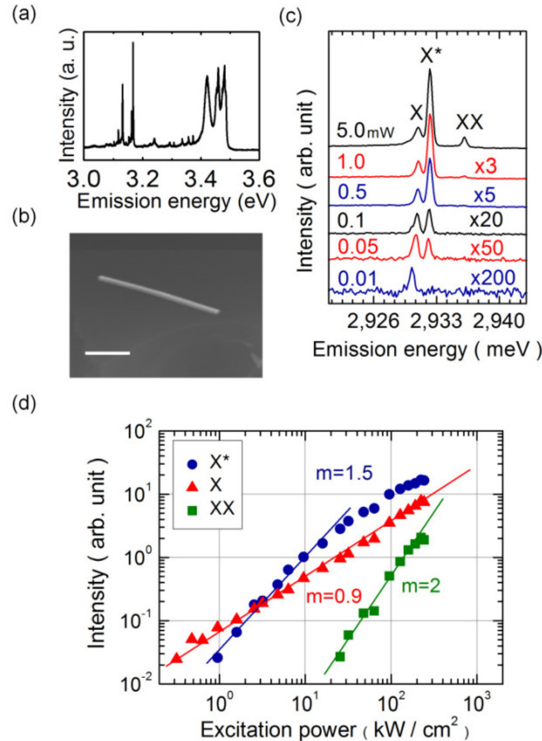

Fig. 3. Optical characterization of single QD. (a) Spectrum of μPL measurement performed on an *as grown* sample. The laser was injected and the emission was detected from the top of the sample and along the c-axis. Since our laser spot-size is 3μm in diameter which is much larger than the rod diameter, both the rod and the underlying columnar part are excited. Thanks to the low-density of rods, isolated single QD emissions can be identified clearly with observed emission energy lower than 3.2 eV. (b) In order to know whether the sharp peaks in (a) come from the QD, single rods were scratched out of the sample and dispersed onto a clean Si surface. SEM images were taken to locate the single nanorod before the μPL experiment. The scale bar is 100 nm. Rod morphology as well as position relative to the metal pattern on the Si can be recorded in the SEM beforehand, and located in the μPL system regarding to the metal pattern. (c-d) Results of μPL measurements for a single nanorod. Excitation power dependent PL spectra reveal three peaks, which can be identified as single exciton(X), biexcition(XX), and trion(X*), according to the power dependence of PL intensity shown in (d). The emission intensities are not saturated as the excitation power varied from 0.2 to 300 kW/cm^2. Solid lines are drawn to guide the eye.

As shown in Fig. 3(a) performed on the as grown sample, single sharp peaks can be observed, thanks to the low rod density. The QD emission here was observed with comparable intensity (not integrated) to the emission of the GaN nanorod. Meanwhile, in order to verify whether the emission came from the QD or the underlying columns, single nanorods were manually scratched and transferred to a piece of silicon chip with a gold metal pattern on top, as shown in Fig. 3(b). The information of location and axial direction of the nanorod and the optical information can be linked by mapping the observation of the SEM results and optical camera images in the PL system. Morphologies of the single rods were carefully recorded before the optical measurement in order to make sure that the single emission peaks come from the top of the isolated rod, instead of the underlying columns. As reported in the literature, typical FWHM of emission from the InGaN QD in rod is 1 to 5 meV [4, 5], and 170 to 1800 μeV [15, 16, 19] for SK dots. In our case, the μPL spectrum of a single QD, as shown in Fig. 3(c), depicted a single sharp peak with a line width of 525 μeV, which reach the detection limit of our equipment. By perform the statistic on μPL

#165391 - $15.00 USD Received 23 Mar 2012; revised 27 Apr 2012; accepted 11 Jun 2012; published 2 Jul 2012
(C) 2012 OSA

measurement over 20 nanorods, we conclude that on average only 1-2 LCs reside in each nanorod. It matches the assumption that the small diameter of rods substantially lowers the chance of multiple LC formations. Excitation power-dependent PL spectra and the corresponding PL intensity (I_{PL}) for each peak as a function of the excitation power (P_{ex}) are shown in Fig. 3(c) and 3(d), respectively.

The power dependence of PL intensity for each peak, characterized by $I_{PL} \propto P_{ex}^{m}$, can be used to identify these emission peaks. The peaks with linear (*m*~1) and quadratic (*m*~2) power dependence can be assigned to the recombination from single excitons (X) and biexcitons (XX), respectively. The peak with superlinear power dependence (*m*~1.5) is likely to arise from trions (X*).

5. Effects of the small wire-diameter

Interestingly, as little as 0.75 meV peak shift was observed across three orders of magnitude of excitation power under very weak excitation and no further shift with increasing excitation power (Fig. 4(a)). Only 0.33 meV peak shift was also observed on the trion peak, which is smaller than the exciton one. It matches the intuition since trion has an extra charge therefore a larger screening effect. The spectral stability indicates very small screening effect and thus a significantly reduced piezoelectric field inside the crystal. It is likely to be the advantage of small rod diameter, which may maximize the strain relaxation via the rod free surfaces. Time-resolved PL measurements on several rods (not shown) also support this finding. The decay lifetimes are ranging from 200 to 650 ps, significantly faster than typical emission from InGaN quantum well, indicative of highly localized electron and hole wave functions in LCs. Polarizations of single QD emissions were also checked as shown in Fig. 4(b). The well-aligned polarization directions of different peaks indicates that the origin of these peaks is the same LC, since the polarization are all determined by the intermediated excitonic state [4, 20] . The exciton and trion peaks are observed with degrees of polarization of 88.9% and 94.4%, respectively. It is reported that Coulomb interactions can affect the polarization of exciton complexes [21], and the negative trion peak has higher degree of polarization than the exciton peak according to the calculation. These emissions exhibited almost total linear polarization, which is essential for implementing quantum key distribution protocols [22].

#165391 - $15.00 USD Received 23 Mar 2012; revised 27 Apr 2012; accepted 11 Jun 2012; published 2 Jul 2012
(C) 2012 OSA

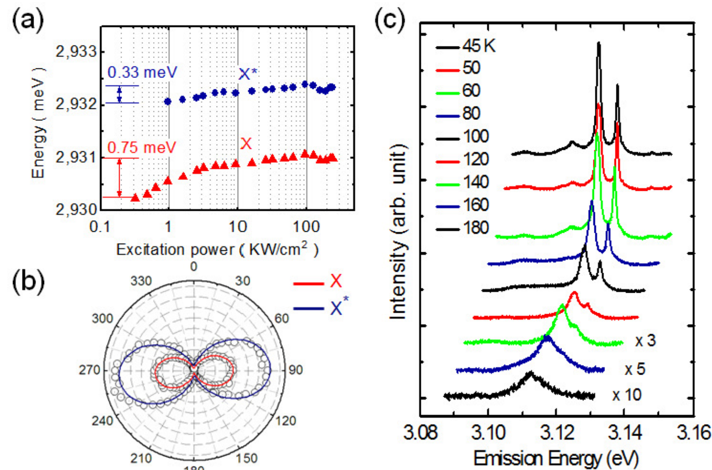

Fig. 4. Power dependent-, polarization dependent-, and temperature dependent- μPL spectra we performed on single QD. (a) With an excitation power-change in three orders of magnitude, exciton and trion peaks shown in Fig. 3 shifted by only 0.75 and 0.33 meV respectively. The peak shifts occur when the power was lower than 3 kW/cm^2, and were almost fixed all the way up to 300 kW/cm^2. It showed very weak but noticeable screening effects inside the QD, thanks to the ignorable strain in the crystal. (b) Polarization dependence measurement of the PL peaks in (a). The numbers denote the rotation-angle of the polarization of the QD emissions. The degree of polarization of 88.9% and 94.4% was detected and calc ulated with the function of P = $(I_{//} - I_{\perp}) / (I_{//} + I_{\perp})$, where $I_{//}$ and $I_{\perp}$ represent the maximum and minimum intensity respectively. The polarization directions of both peaks are well aligned, showing the same origin of the emissions. (c) Temperature-dependent PL spectra from a single QD. It is observed that QD emissions can be detected in the high temperature. The highest tolerant temperate is 180K.

Temperature dependent μPL was also performed in order to investigate the thermal tolerance of the QDs, as shown in Fig. 4(c). Single LC emissions could be identified up to 180 K, the highest emission temperature of single InGaN SK dot and single LC that have been reported to date [9, 23–25]. Although InGaN has been commercially utilized owing to its high emission efficiency at room temperature, so far single LC emission could be detected only at low temperatures. Therefore, with the capability of characterizing single LC, both structurally and optically, the present structure can also be a system for investigating the origin of the InGaN LC-emission.

6. Conclusion

In conclusion, single InGaN/GaN QDs embedded in narrow nanorods have been successfully grown by using MBE, without the requirement of extensive processing steps. On average only 1-2 InGaN LCs are present in the InGaN layer of each individual rod. A sharp, bright, highly polarized, and background-free single QD emission observed in the visible range is possibly due to the small rod diameter, high structural quality and strain relaxation of the rod surface. The structure gives a tentative direction for electrically-driven device fabrication by utilizing the properties of good rod alignment, low rod density, ease-of-dope barrier layer, and the capability of microcavity shell fabrication and wafer-scale mass production.

Acknowledgments

This work is financially supported by Ministry of Education and National Science Council in Taiwan. We would like to thank professor Per Olof Holtz and Fredrik Karlsson in Linkoping University (Sweden), and professor Yasushi Nanishi and Tsutomu Araki in Ritsumeikan University (Japan) for valuable suggestions. The TEM and UV lithography were performed at the Centre of Core Facilities for Nanoscience and Facilities, Academia Sinica, Taiwan.

(C) 2012 OSA